Supplementary Information

Supplementary Data

Figure S1, Related to Figure 1. Autonomic activity at rest in HC, bvFTD and AD. A) Heart rate variability, measured by CVI (left) and logHRV (right). * signifies significant differences between groups at $p < 0.05$. B) Heart rate, measured by mean IBI, and C) skin conductance level in HC, bvFTD and AD. Error bars signify standard error of the mean.

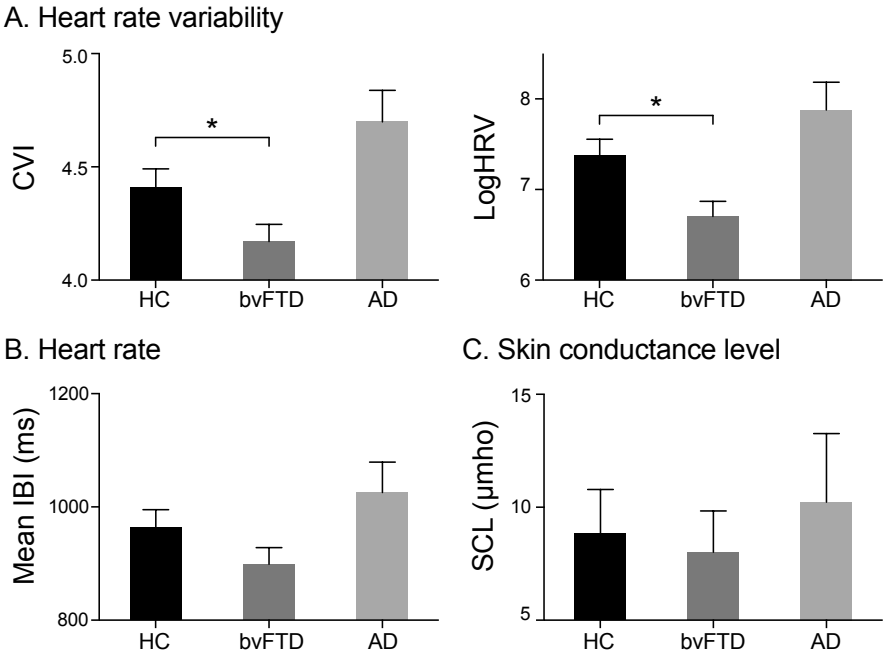

Figure S2, Related to Figure 2**.** Changes in Pearson correlation coefficients between the mean continuous HRV and the CVI when using different sliding windows (top). The relationship between the CVI, derived using the Lorenz plot (see Methods) and mean HRV, derived using the 18 second sliding window, is shown (all subjects, bottom).

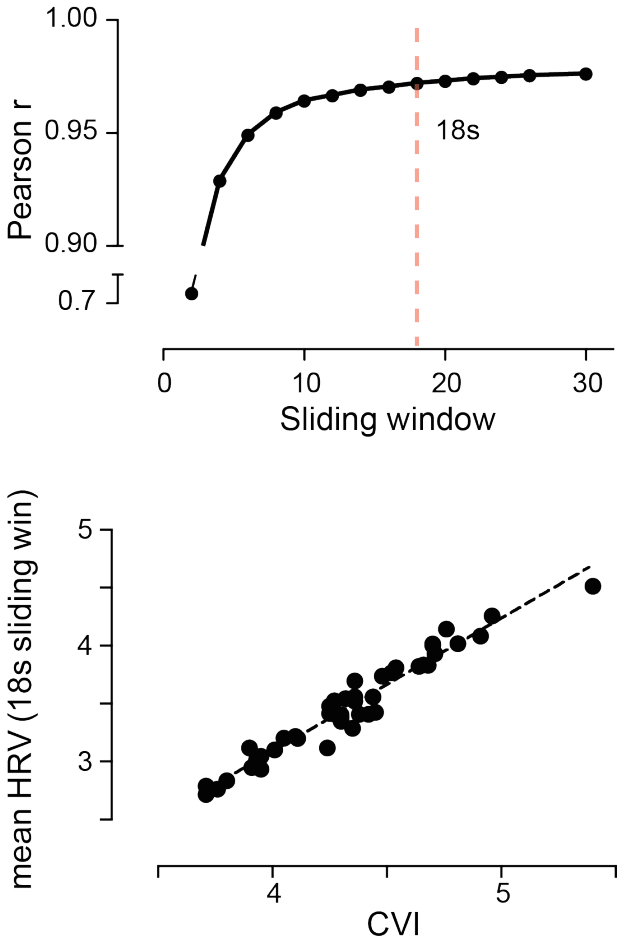

Figure S3, Related to Figure 3. Post hoc analyses of correlation between functional connectivity and CVI in bvFTD (orange) and HC (white) separately. Results from selected clusters are shown for connectivity analyses based on the right FI seed (A), left FI seed (B) and whole brain voxelwise connectivity (degree centrality). Data are shown for visualization purposes only, to illustrate that both bvFTD and HC groups contributed to the relationships between connectivity and CVI identified across all subjects (Figure 3).

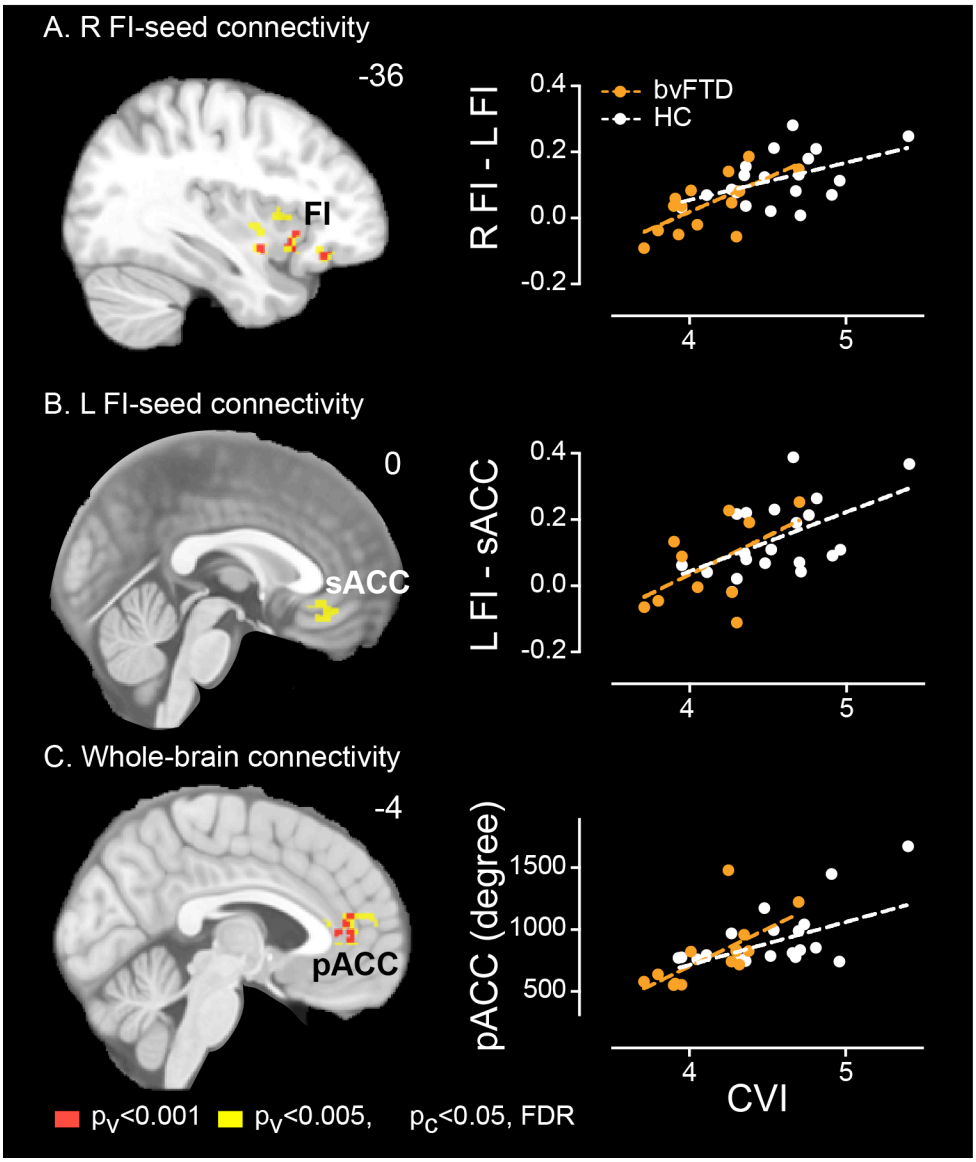

Figure S4, Related to Figure 4. A. Structural differences between bvFTD and HC. p < 0.001 (yellow) and FWE corrected p < 0.05 (red) for peak height. B. Lack of correlation between the CVI and gray matter intensity in the left and right sides of the salience network.

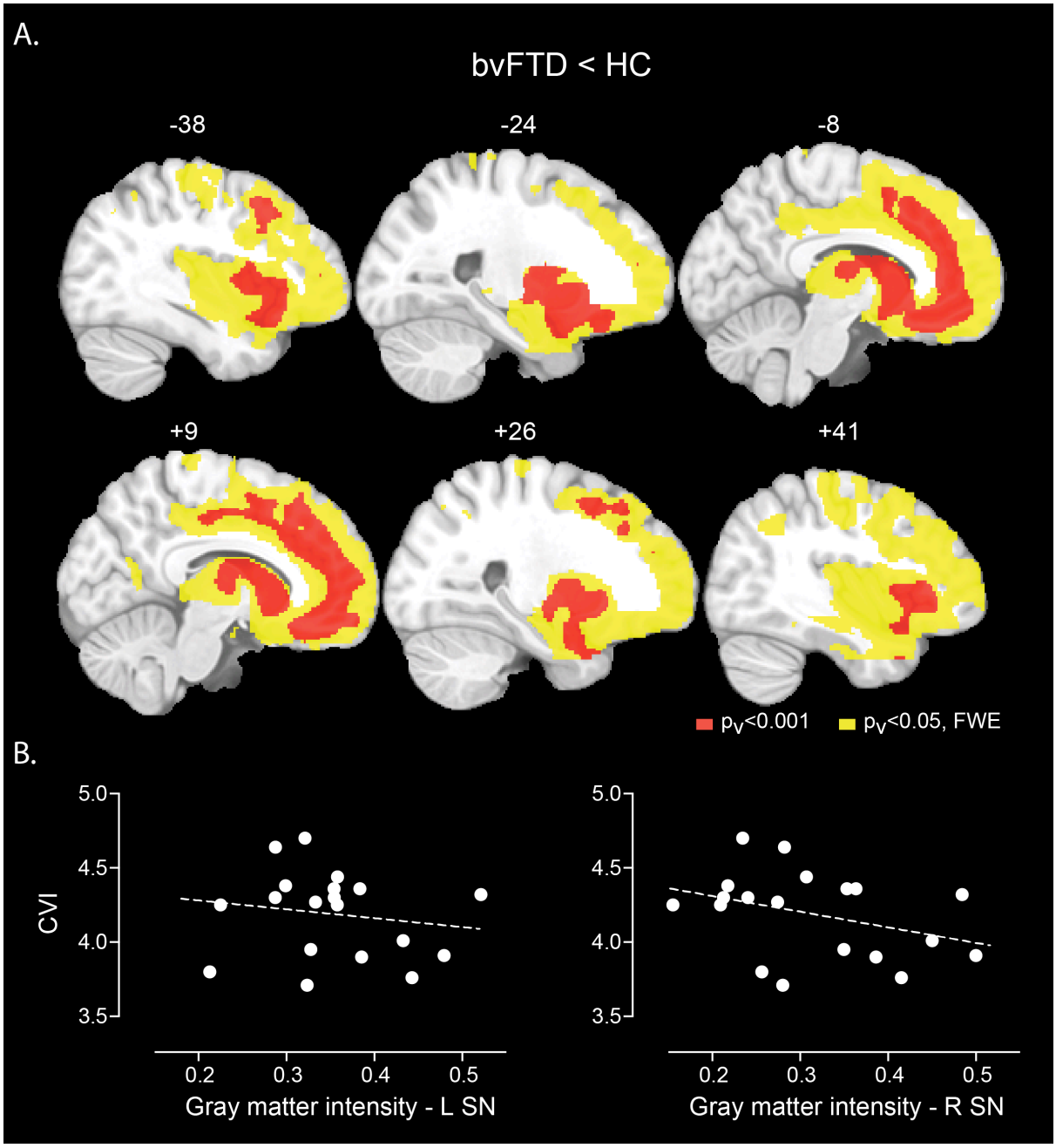

Figure S5, Related to Figure 1**.** Autonomic activity during eyes-closed and eyes-open conditions in HC. A) Heart rate variability, measured by CVI (left) and logHRV (right), B) Heart rate, measured by mean IBI, and C) skin conductance level. Error bars signify standard error of the mean. In healthy controls, cardiac vagal tone decreased and SCL increased significantly between eyes-closed and eyes-open conditions (paired t-test, $p < 0.05$). These results are consistent with the increased alertness associated with eyes-open condition (1, 2), supporting the physiological validity of these autonomic metrics.

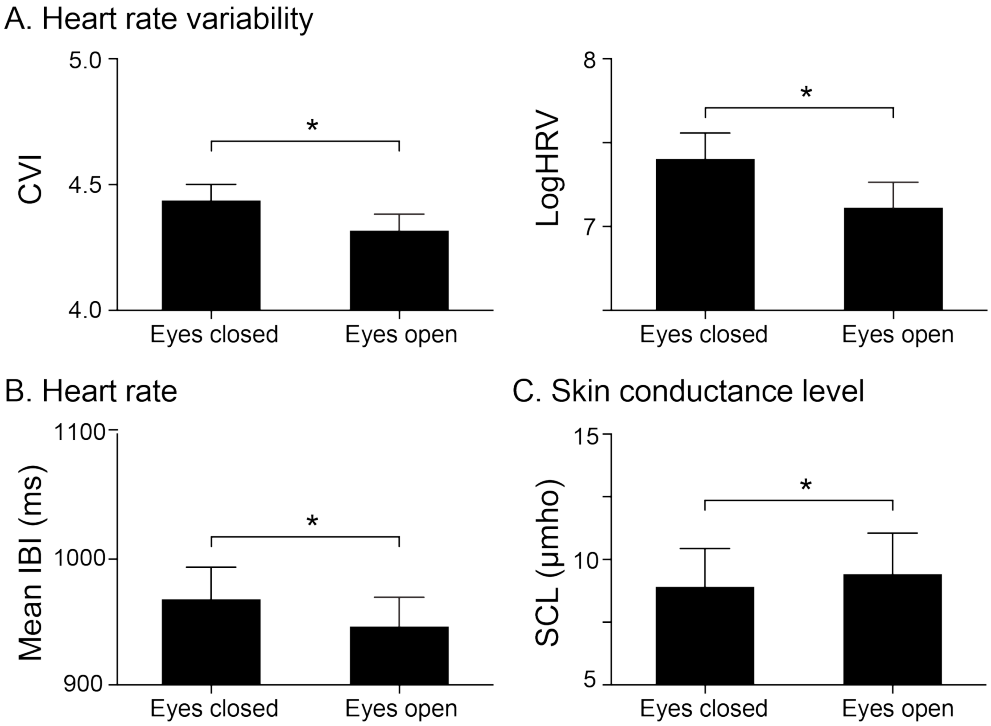

Table S1, Related to Figure 1.
Group differences between HC and bvFTD analyzed by GLM, univariate analysis of variance, with DX as the main effect and gender, BMI, age, and handedness as covariates. Table shows the F statistics and p value corresponding to each factor.

	DX	Gender	BMI	Age	Handedness
MeanIBI, ms	0.15, 0.70	0.51, 0.48	0.21, 0.65	0.39, 0.54	0.20, 0.6
CVI	5.13, 0.03	0.11, 0.74	1.93, 0.18	0.12, 0.74	0.11, 0.75
RSA	9.96, 0.04	0.08, 0.78	1.93, 0.18	0.70, 0.41	0.25, 0.63
LogHRV	6.04, 0.02	0.46, 0.51	3.83, 0.06	1.29, 0.27	0.32, 0.58

Table S2, Related to Table 1.
Demographics characterizing the gender-balanced and unmedicated HC and bvFTD groups used in the follow-up analyses. Group differences analyzed by two sample t tests.

	HC	bvFTD	HC vs. bvFTD
	Mean (SD)	Mean (SD)	t, p
Age, years	60.15 (9.68)	62.31 (3.84)	-0.77, 0.45
Gender (M:F)	9:5	9:5	-
Handedness (R:L)	13:1	13:1	-
Education, years	16.79 (2.00)	16.93 (2.34)	-0.17, 0.86
Mean IBI, ms	969.55 (140.64)	892.86 (133.83)	1.48, 0.151
CVI	4.46 (0.35)	4.15 (0.24)	2.72, <0.05
RSA	5.58 (0.85)	4.98 (0.60)	2.56, <0.05
LogHRV	7.46 (0.77)	6.65 (0.54)	3.21, <0.005

Table S3, Related to Table 1
Demographics and autonomic variables in HC, bvFTD and AD, analyzed by ANOVA

	HC (19)	bvFTD (20)	AD (8)	Group differences
	Mean (SD)	Mean (SD)	Mean (SD)	F or $\chi 2$, p
Age, years	59.5 (12.2)	60.1 (7.3)	57.6 (6.9)	0.19, 0.83
Gender (M:F)	9:10	14:6	4:4	2.26, 0.32
Handedness (R:L)	17:2	19:1	8:0	1.15, 0.56
Donepezil (N:Y)	19:0	17:3	3:5	15.7, < 0.001
Education, years	16.9 (1.9)	16.1 (2.8)	17.5 (1.4)	1.25, 0.30
Mean IBI, ms	965.8 (127.0)	901.0 (130.5)	1007.4 (81.6)	2.60, 0.09
CVI	4.5 (0.3)	4.2 (0.3)	4.6 (0.5)	6.60, 0.003
RSA	5.8 (0.9)	4.9 (0.8)	5.6 (1.4)	4.36, 0.006
LogHRV	7.6 (0.6)	6.7 (0.7)	7.8 (1.0)	9.76, < 0.001
CSI	1.8 (0.7)	1.8 (0.7)	2.0 (0.6)	0.99, 0.38

SCL, μmho	10.4 (7.5)	8.0 (6.5)	8.0 (8.5)	0.31, 0.73
CDR, Total	0.0 (0.0)	1.3 (0.7)	0.9 (0.2)	41.71, < 0.001
CDR, sum of boxes	0.0 (0.0)	7.5 (3.4)	4.9 (1.7)	46.30, < 0.001
MMSE (max 30)	29.6 (0.6)	24.4 (4.0)	24.1 (3.4)	17.58, < 0.001
Verbal Ability	5.9 (0.4)	4.8 (1.5)	5.1 (1.1)	3.50, 0.042
Syntax comprehension	4.9 (0.3)	3.9 (1.0)	3.3 (1.3)	11.39, < 0.001
Reading, irregular	5.5 (1.9)	5.4 (1.2)	5.6 (1.1)	0.41, 0.959
Calculation (max 5)	4.9 (0.2)	3.3 (1.4)	3.3 (1.5)	13.24, < 0.001
Digit span (forward)	7.6 (1.3)	5.5 (1.4)	5.4 (1.1)	14.95, < 0.001
Digit span (backward)	5.7 (1.2)	3.7 (1.8)	3.6 (1.6)	10.25, < 0.001

Table S4, Related to Figure 1.
Group differences between HC, bvFTD and AD analyzed by GLM, univariate analysis of variance, with DX as the main effect, and gender, donepezil, age, and handedness are covariates. Table shows F statistics and p value corresponding to each factor.

	DX	Gender	BMI	Donepezil	Age	Handedness
Mean IBI	0.64, 0.43	0.10, 0.75	0.00, 0.99	0.17, 0.68	1.07, 0.31	0.25, 0.62
CVI	7.40, 0.004	0.00, 0.90	0.53, 0.47	0.04, 0.85	2.08, 0.16	0.07, 0.79
RSA	10.20, 0.003	0.05, 0.83	0.98, 0.33	2.09, 0.16	0.62, 0.44	0.66, 0.42
LogHRV	9.72, 0.002	0.01, 0.94	0.08, 0.78	0.77, 0.37	2.68, 0.09	0.03, 0.86

Table S5, Related to Figure 2 and 3.
MNI coordinates for cluster peaks in Figures 2 and 3.

Brain Regions	**Side**	**MNI**			**t-values**
		x	**y**	**z**	
Functional activations with HRV (Fig. 2A)					
MCC*	L	-10	4	42	6.04
Insula*	L	-36	-2	-6	5.37
Insula*	L	-36	8	-6	5.35
Postcentral*	L	-60	0	18	5.04
ACC*	R	10	20	28	4.41
IFG	R	50	18	-10	4.94
HC > bvFTD (Fig. 2B)					
ACC#	L	-2	32	-4	4.71
Insula#	L	-32	10	-18	3.62
Correlation with R FI-seeded connectivity network (Fig. 3A)					
Insula*	L	-34	8	-10	5.42

IFG*	L	-50	42	-2	5.35
STG	L	-50	-2	-10	5.68
Insula	L	-38	10	6	5.11
Cerebellum	R	12	-54	-8	4.60
MOG	R	2	36	-14	4.13
Correlation with L FI-seeded connectivity network (Fig. 3B)					
Linual*	L	-10	-72	-6	6.63
IFG*	L	-38	28	-12	5.09
Insula*	L	-36	20	-6	4.86
MCC*	L	-10	-22	34	4.84
MCC	R	10	-22	36	4.98
Fusiform	R	32	-58	-8	4.88
IOG	R	40	-70	-6	4.60
Posterior-medial frontal	L	-4	-16	50	4.33
IFG	L	-40	32	2	4.09
Temporal Pole	R	40	18	-30	4.06
Correlation with whole-brain connectivity network (Fig. 3B)					
Putamen*	L	-24	12	6	6.07
ACC*	L	-8	40	4	4.58
Insula*	L	-34	10	-8	4.57
MFG	L	-40	42	22	5.81
Insula	R	36	12	-8	4.79
SMG	R	10	50	36	4.79
Precentral	L	-58	6	22	4.13

ACC = Anterior Cingulate Cortex; IFG: Inferior Frontal Gyrus; IOG = Inferior Occipital Gyrus; MCC = Middle Cingulate Cortex; MFG = Middle Frontal Gyrus; MOG = Middle Occipital Gyrus; SMG = Superior Medial Gyrus; SMG = Superior Temporal Gyrus. *p<0.001 or <0.005, #p<0.01 for voxel height.

Supplementary Experimental Procedures

Head motion assessment

The motion parameters estimated in the realignment process were used to compute the magnitude of head motion during each scan. Based on the volume-to-volume changes in motion parameters, mean root-mean-square (RMS) values were calculated for translation and mean Euler angles for rotation, as these summary metrics have been shown to correlate with network connectivity strength (3). One of the 19 HC and 3 of the 17 bvFTD subjects had greater than 2 mm in absolute translational motion and were excluded from further imaging analyses. The remaining bvFTD and HC groups did not differ in translational (2-sample t tests, p = 0.23) or rotational movement (p = 0.06). To further reduce potential impact of motion artifact, we included RMS values as nuisance covariates in group-level imaging analyses.

Image acquisition

Structural and functional MR images were acquired at the UCSF Neuroscience Imaging Center, on a 3 Tesla Siemens TIM Trio scanner equipped with a 12-channel receiver head coil. A volumetric magnetization prepared rapid gradient echo (MPRAGE) sequence was used to obtain 1x1x1 mm^3 T1-weighted images of the entire brain (TR/TE/TI = 2300/3/900 ms, flip angle of 9 degrees, a bandwidth of 240 Hz/pixel, sagittal orientation with a FOV = 256 x 240 mm and 160 slices). Task-free fMRI scans were obtained using 36 axial slices (3

mm thick) parallel to the plane connecting the anterior and posterior commissures and covering the whole brain using a T2*-weighted gradient echo–echo planar sequence (TR/TE = 2000/27 ms, flip angle 80°; FOV = 230 × 230 mm; matrix size = 92 × 92; 3 mm slices with 2.5 × 2.5 × 3 mm resolution; slice gap = 0.6 mm). All subjects underwent two scanning sessions (each lasting 8 minutes with 240 images) during which they were instructed only to remain awake with their eyes open in the first session and eyes closed in the second.

Image preprocessing and analysis

Structural Imaging

T1-weighted images were segmented using VBM8. The gray matter images were further normalized into Montreal Neurological Institute (MNI) space (high-dimensional DARTEL normalization), modulated by the Jacobian determinant of the non-linear only, and smoothed with an 8 mm full-width at half-maximum Gaussian kernel. These resulting images were used as nuisance covariates for voxel-wise atrophy correction of functional imaging analyses, and to extract gray matter volumes for calculating lateralization indices, as described below. We also performed a two-sample test between HC and bvFTD using VBM8, to examine the extent of atrophy presented in patients with bvFTD.

Functional Imaging

After discarding scans acquired in the first sixteen seconds to allow for quasi-equilibrium in longitudinal magnetization to be achieved, functional images were realigned and unwarped, slice-time corrected, co-registered, spatially normalized to standard space and smoothed with a 4 mm full-width at half-maximum Gaussian kernel using SPM8. Unwarping was performed to reduce artifacts due to movement-by-deformation interactions. Co-registration was performed between the mean EPI images and the subject's own T1-weighted image, and normalization and smoothing were carried out in an interactive process using the DARTEL toolbox. Subsequently, the functional images were re-sampled at a voxel size of 2 mm^3. These preprocessed images were then used for seed-based ROI and whole brain voxel-wise connectivity analyses, as described in the following sections.

Seed-based ROI analyses

Briefly, after temporal filtering with a band-pass filter ($0.0083 < f < 0.15$ Hz), the average voxel-wise time series from each ROI was detrended and used as a covariate of interest in a whole-brain, linear regression, statistical parametric analysis. White matter, CSF, non-brain (voxels that are not gray matter, white matter or CSF) timeseries and six motion parameters were included as nuisance regressors, as shown to produce reliable intrinsic connectivity measures (4). This procedure generated a statistical parametric map from each scan session, where each voxel was scored based on its BOLD signal correlation with the seed ROI used in the analysis (referred to throughout the paper as "connectivity"). The ICN map for each subject was entered into second-level, random-effects regression analyses seeking brain-behavior relationships.

Gray matter intensity correction

To further examine whether the observed group differences and correlations in functional maps were related to gray matter atrophy, gray matter intensity correction was performed using the Biological Parametric Mapping (BPM) toolbox (5), on 1) the two-sample test on BOLD-HRV correlation maps between HC and bvFTD, 2) the correlational analyses between seed-based maps and CVI, and the correlational analysis between the whole brain connectivity centrality maps and CVI. These analyses were re-assessed where the voxel-wise gray matter intensity maps, i.e., the normalized and modulation structural images, were included as covariates,

Supplementary References

1. Barry RJ, Clarke AR, Johnstone SJ, Magee C a, Rushby J a (2007) EEG differences between eyes-closed and eyes-open resting conditions. *Clin Neurophysiol* 118:2765–73.

2. Hori K et al. (2005) Influence of sound and light on heart rate variability. *J Hum Ergol (Tokyo)* 34:25–34.

3. Van Dijk KR, Sabuncu MR, Buckner RL (2011) The Influence of Head Motion on Intrinsic Functional Connectivity MRI. *Neuroimage*:1–8.

4. Guo CC et al. (2012) One-year test-retest reliability of intrinsic connectivity network fMRI in older adults. *Neuroimage* 61:1471–83.

5. Casanova R et al. (2007) Biological parametric mapping: A statistical toolbox for multimodality brain image analysis. *Neuroimage* 34:137–43.